

Geographic variation in morphology in the Mohave Rattlesnake (*Crotalus scutulatus* Kennicott 1861) (Serpentes: Viperidae): implications for species boundaries

JESSICA A. WATSON¹, CAROL L. SPENCER², DREW R. SCHIELD³, BRETT O. BUTLER⁴, LYDIA L. SMITH², OSCAR FLORES-VILLELA⁴, JONATHAN A. CAMPBELL³, STEPHEN P. MACKESSY⁵, TODD A. CASTOE³ & JESSE M. MEIK^{1,6}

¹Department of Biological Sciences, Tarleton State University, 1333 W. Washington Street, Stephenville, Texas, 76402 USA.

²Museum of Vertebrate Zoology, 3101 Valley Life Sciences Building, University of California, Berkeley, California 94720 USA.

³Department of Biology, 501 S. Nedderman Drive, University of Texas at Arlington, Arlington, Texas 76019 USA.

⁴Museo de Zoología, Department of Evolutionary Biology, Facultad de Ciencias, Universidad Nacional Autónoma de México, External Circuit of Ciudad Universitaria, México City 04510, Mexico.

⁵School of Biological Sciences, 501 20th Street, University of Northern Colorado, Greeley, Colorado 80639 USA.

⁶Corresponding author. E-mail: meik@tarleton.edu

Abstract

The Mohave Rattlesnake (*Crotalus scutulatus*) is a highly venomous pitviper inhabiting the arid interior deserts, grasslands, and savannas of western North America. Currently two subspecies are recognized: the Northern Mohave Rattlesnake (*C. s. scutulatus*) ranging from southern California to the southern Central Mexican Plateau, and the Huamantla Rattlesnake (*C. s. salvini*) from the region of Tlaxcala, Veracruz, and Puebla in south-central Mexico. Although recent studies have demonstrated extensive geographic variation in venom composition and cryptic genetic diversity in this species, no modern studies have focused on geographic variation in morphology. Here we analyzed a series of qualitative, meristic, and morphometric traits from 347 specimens of *C. scutulatus* and show that this species is phenotypically cohesive without discrete subgroups, and that morphology follows a continuous cline in primarily color pattern and meristic traits across the major axis of its expansive distribution. Interpreted in the context of previously published molecular evidence, our morphological analyses suggest that multiple episodes of isolation and secondary contact among metapopulations during the Pleistocene were sufficient to produce distinctive genetic populations, which have since experienced gene flow to produce clinal variation in phenotypes without discrete or diagnosable distinctions among these original populations. For taxonomic purposes, we recommend that *C. scutulatus* be retained as a single species, although it is possible that *C. s. salvini*, which is morphologically the most distinctive population, could represent a peripheral isolate in the initial stages of speciation.

Key words: Biogeography, external morphology, linear morphometry, species delimitation, Pleistocene, taxonomy

Introduction

Current genetic diversity in the western North American vertebrate fauna has been shaped largely by Miocene and Pliocene orogenesis and subsequent Pleistocene glacial cycles (Douglas *et al.* 2006; Riddle & Hafner 2006; Man-tooth *et al.* 2013; Myers *et al.* 2016). During glacial periods, geographic distributions of widely distributed taxa were fragmented and reduced, starting the process of divergence in isolation. However, during interglacial periods and after the last glacial maximum, populations have expanded into secondary contact, providing opportunities for gene flow among once isolated populations (Wood *et al.* 2008, 2013; Myers *et al.* 2016). Although these cyclical global events likely influenced evolutionary histories of co-distributed taxa in similar ways, the extent to which speciation has occurred across disparate lineages has been equivocal (Schield *et al.* 2015). Regardless, the complex but partially tractable histories and demographics of these groups makes them ideal candidates for studying the nuances of speciation in vertebrates.

The Mohave Rattlesnake (*Crotalus scutulatus* Kennicott 1861) is distributed continuously throughout the inte-

rior arid zone of southwestern North America from southern California southeast to southern Mexico. Two poorly defined subspecies are currently recognized: the Northern Mohave Rattlesnake (*C. s. scutulatus* Gloyd 1940) occurs from southeastern California to the southern Central Mexican Plateau, and the Huamantla Rattlesnake (*C. s. salvini* Gloyd 1940) occurs in the matorral region from the eastern passes of the Trans-Volcanic Axis of State of Mexico, Tlaxcala, and Veracruz, south into the semiarid upper Balsas Basin (Gloyd 1940; Klauber 1972; Campbell & Lamar 2004). Over this expansive distribution, these snakes inhabit desert flatlands, desert scrublands, arid grasslands, mesquite savannas, and oak scrublands. The taxonomic history is convoluted because early researchers considered *C. scutulatus* to be an “annectant” form, intermediate between *C. viridis* Rafinesque 1818 and *C. atrox* Baird and Girard 1853 (Klauber 1930; Gloyd 1940). Due to the extensive geographic variation in venom composition across populations of *C. scutulatus*, including populations with neurotoxic, hemorrhagic, and mixed venom phenotypes, the species has been subjected to considerable research focusing on the various roles that diet, climate, and neutral processes have played in shaping venom phenotypes (Strickland *et al.* 2018a,b; Zancolli *et al.* 2019). Collectively, these studies have implicated local adaptation, rather than neutral processes, as a dominant factor driving fine-scale spatial variation in venom composition across its range.

Crotalus scutulatus also was the focus of recent molecular phylogenetic studies, which inferred four well-supported and divergent mitochondrial clades that correspond with populations in the Mohave-Sonoran Desert, Chihuahuan Desert, Central Mexican Plateau (hereafter Central Plateau), and southern Mexican matorral (currently recognized as *C. s. salvini*), respectively (Schield *et al.* 2018, 2019; Strickland *et al.* 2018b; Fig. 1). Schield *et al.* (2018) further demonstrated that nuclear genetic data additionally support these four distinct lineages, and provide evidence for past and/or ongoing gene flow between all geographically adjacent lineages. Accordingly, despite genetic evidence for as many as four distinct lineages, the appropriate taxonomic status of these lineages remains an open question.

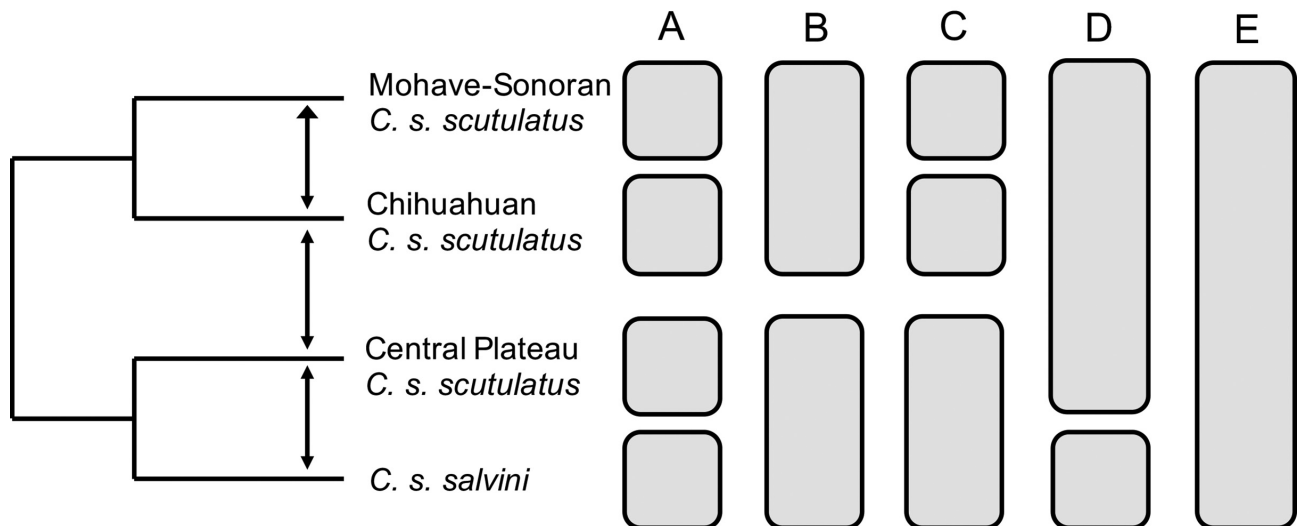


FIGURE 1. Mitochondrial phylogeny of *Crotalus scutulatus* lineages reproduced from Schield *et al.* (2018), with arrows showing inferred gene flow between adjacent clades. Grey bars represent hypotheses of species limits corresponding to (A) a four-species model where each mitochondrial clade is a species, (B) a two-species model where the deepest mitochondrial split coincides with species (i.e., “expanded *salvini*” hypothesis), (C) a three-species model where the deepest nuclear splits coincide with species (i.e., an alternative “expanded *salvini*” hypothesis), (D) a two-species model where current subspecies are elevated to species, and (E) a one-species model where *C. scutulatus* is recognized as a single species. Different sizes of arrowheads indicate direction of asymmetric gene flow between adjacent clades.

Here we investigate morphological variation across the distribution of *Crotalus scutulatus* and evaluate our inferences in context of recent molecular studies (Schield *et al.* 2018; Strickland *et al.* 2018b) to evaluate the taxonomic status of the species. Because our purpose was to interpret phenotypic patterns within the context of previous genetic studies, we considered five alternative species hypotheses (Fig. 1): (A) each of four putative genetic lineages represents a unique species; (B) a more conservative hypothesis whereby the deepest lineage divergence (at the boundary between Chihuahuan and Central Plateau populations) divides *C. scutulatus* into two species (i.e., an “expanded *salvini*” concept); (C) an alternative “expanded *salvini*” concept, but which further splits Mohave-

Sonoran and Chihuahuan lineages, in congruence with the deepest nuclear splits (Schield *et al.* 2018); (D) each subspecies (as currently defined geographically) represents a species; or (E) *C. scutulatus* is maintained as a single species. Based on previous analyses of genetic data, each of these hypotheses has some merit, but a more definitive taxonomic assessment would benefit from a perspective from morphological variation.

Materials and methods

Species delimitation criteria. Most species concepts assume some level of evolutionary independence between species lineages, which ultimately results from genomic divergence and accumulation of reproductive barriers (Coyne & Orr 2004; Wu & Ting 2004). Under the perception of species as meta-population lineages, prezygotic reproductive barriers are not a strict requirement among recently diverged species, but are contingent properties that could signal divergence along with other properties (de Queiroz 1998, 2007). Therefore, some level of gene flow might occur between nascent species, but should not be sufficient to hinder their independence as separate evolutionary lineages (de Queiroz 2007; Feder *et al.* 2012; Nosil & Feder 2012). Phenotypic data are useful not only for aiding physical recognition of species, but they also coarsely surrogate for genetic divergence as long as phenotypes are heritable. Here we follow a multivariate phenotypic cohesion criterion for evaluating whether morphologically cohesive groups correspond geographically with genetic groups or combinations of groups (i.e., whether shifts in distributions of multiple variables correspond with phylogeographic breaks). Alternatively, phenotypic traits might show clinal or mosaic variation across clades or even discordant variation, where phenotypically distinctive groups do not correspond with phylogeographic patterns. The rationale for phenotypic cohesion of multiple characters follows the basic evolutionary model of Fisher (1918), where continuous or quasi-continuous traits of individual species should be normally distributed under conditions approximating Hardy-Weinberg equilibrium (Templeton 2006; Cadena *et al.* 2018). Therefore, mixed normal distributions within a sample would be indicative of multiple potential species.

Phenotypic data. We collected a series of one qualitative, ten meristic, and eleven morphometric characters for 347 alcohol-preserved specimens of subadult and adult *Crotalus scutulatus* from throughout its distribution. All specimens examined are accessioned in natural history collections in the United States, Mexico, and Great Britain (Appendix 1) and, when available, museum abbreviations follow Sabaj (2016). We recorded latitude and longitude for specimens using VertNet, Arctos, and collections data whenever possible, and georeferenced specimens from qualitative locality data when coordinates were not available using Google Earth. We followed Klauber (1972) Gutberlet and Harvey (2002), and Campbell and Lamar (2004) for terminology of morphological characters, and provide character descriptions and abbreviations in Appendix 2. Our choice of characters was based on previous studies of variation in the *C. viridis*-*scutulatus* complex, as well as an attempt to minimize strong dependence between some standardized scale counts. We determined sex by scoring presence of hemipenes. Total length and tail length were measured to nearest millimeter using a string and a metric ruler; all other morphometric characters were measured with digital calipers to the nearest 0.1 mm. We obtained snout-vent length (SVL) by subtracting tail length (CL) from total length (TL), and then subtracted head length (HL) from SVL to obtain body length (BL).

Among rattlesnakes, *Crotalus scutulatus* tends to have comparatively low subdivision of head scales in both the prefrontal and parietal regions, and approaches species of *Sistrurus* in this respect (Gloyd 1940). Both *C. s. scutulatus* and *C. s. salvini* have few intersupraocular scales (usually a minimum of two spanning a row), and have a distinctive large crescentic scale at the medioposterior border of each of the supraoculars (Cardwell 2016; Figs. 2A–B). With respect to subspecies distinctions, previous authors have indicated that *C. s. salvini* differs from *C. s. scutulatus* in having less subdivision of crown scales, distal tail bands that are similar in color to dorsal blotches versus distal tail bands that are notably darker, and dorsal blotches that lack a distinct border of pale white scales (Klauber 1930; Gloyd 1940; Campbell & Lamar 2004). For each specimen, we scored whether pale blotch borders were distinct, indistinct, or absent (Figs. 2C–E).

Statistical analyses. Because we evaluated morphological variation in the context of previous molecular studies, we first assigned specimens of *Crotalus scutulatus* to one of four putative genetic lineages defined by Schield *et al.* (2018) based on locality of origin (Fig. 3). For our full dataset, we summarized geographic variation in individual quantitative characters across each putative genetic lineage. Because we defined condition of blotch borders as a qualitative character, we analyzed this trait separately using a Pearson chi-squared test of independence, which

evaluated whether frequencies of individuals assigned to each category were independent across putative genetic lineages. For all multivariate statistical analyses, we used a subset of individuals for which we had complete morphometric and meristic data ($n = 243$). Prior to analyses, we log-transformed morphometric variables, and excluded SVL and TL in order to include HL independently in analyses, and because these measurements were used to derive BL and CL. We first applied principal components analysis (PCA) using the correlation matrix to reduce dimensionality of our dataset and to evaluate gradients of morphological variation across the range of *C. scutulatus* in the context of correlated shifts in character values. We retained for further analysis all principal components that explained more than 5% of the total variation in the dataset. We plotted PC factor scores for the first three PC axes to evaluate whether discrete breaks in morphology were evident among lineages. We also applied the same character set to linear discriminant analysis (LDA) to determine whether training a model on labeled data (i.e., putative genetic lineages) would provide better separation of groups in multidimensional space (i.e., ‘morphospace’). From LDA, we also extracted the posterior probability of assignment of individuals to each lineage and averaged these values as a summary metric of discrimination among groups (see Meik *et al.* 2018). Because ordination of morphospace is subjective regardless of methodology, we also used model-based clustering to determine the optimal number and assignment of groups present in our dataset without *a priori* assumptions of classification (Fraley & Raftery 2007). Model-based clustering uses Gaussian mixture models (GMM) and Bayesian Information Criterion (BIC) to evaluate models with different numbers of groups (K), each with different multivariate volumes, orientations, and shapes (e.g., ellipsoidal, spherical, diagonal).

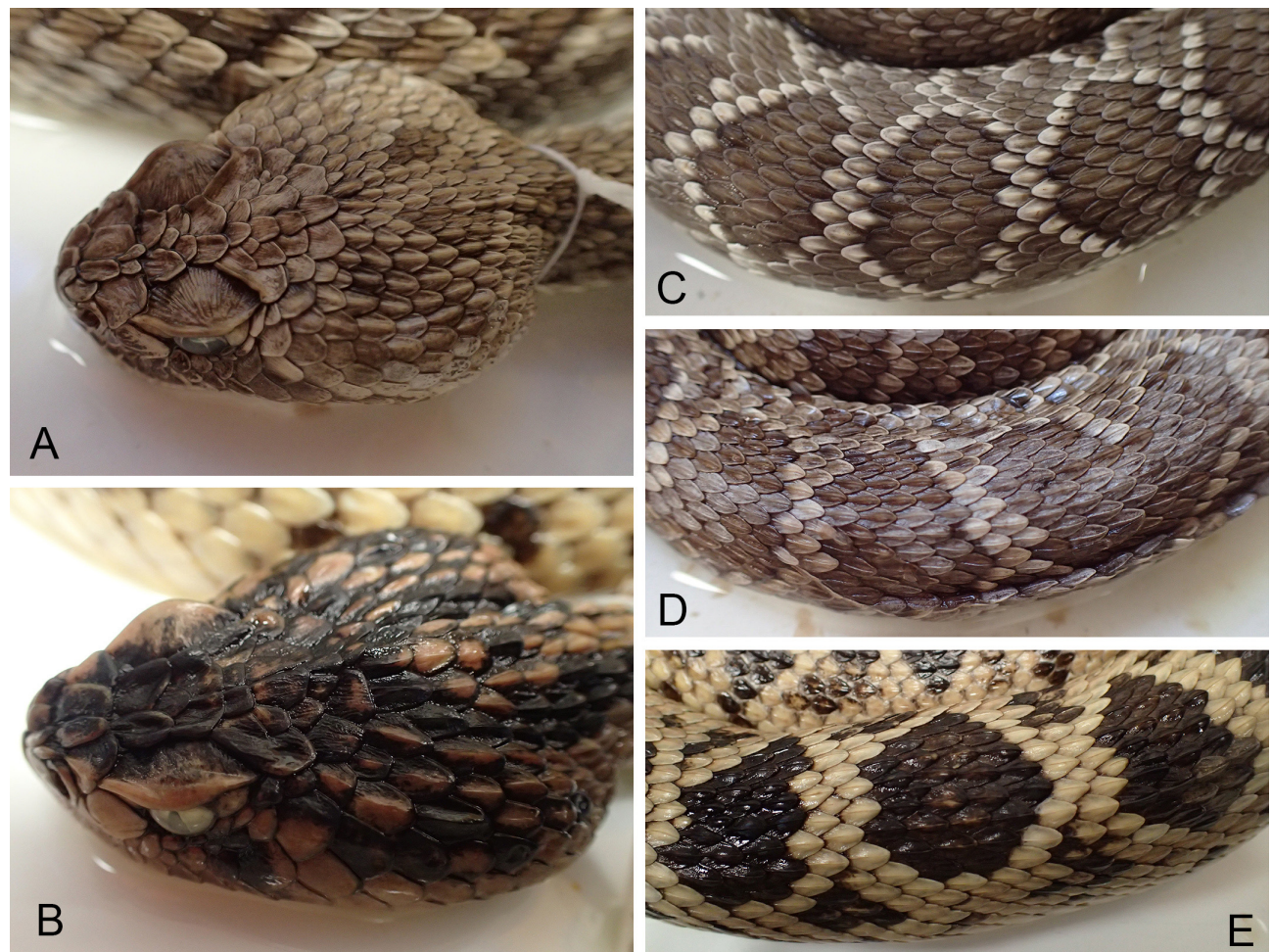


FIGURE 2. Oblique views of head scalation in (A) *Crotalus scutulatus scutulatus* (MVZ 275547) and (B) *C. s. salvini* (MVZ 275545), and representative examples of dorsal blotch condition as scored in this study: (C) pale dorsal blotch borders distinct (MVZ 275562), (D) pale dorsal blotch borders indistinct (MVZ 102990), and (E) pale dorsal blotch borders absent (MVZ 275545).

To evaluate general patterns in phenotypic variation among lineages while simultaneously accounting for sexual dimorphism, we used a series of two-way ANOVAs with genetic lineage and sex as the independent variables

and PC factor scores for the first five PC axes as the dependent variable. We regressed factor scores for the first five PCs against latitude and longitude using least squares linear regression to determine whether correlated shifts in character distributions showed continuous variation or corresponded with geographic breaks between adjacent lineages. To more generally evaluate an “isolation-by-distance” model using our morphological data matrix, we further converted raw data into a Mahalanobis distance matrix and performed a mantel test against geodesic distances using 99,999 permutations. Because relative head size is an important taxonomic trait in some rattlesnake groups (e.g., *C. mitchellii* complex; Meik *et al.* 2015) and also indicates potential shifts in diet, we further analyzed the scaling relationship between HL (log mm) and BL (log mm) across *C. scutulatus* lineages using ANCOVA after confirming homogeneity of slopes. We used the MASS package to perform LDA (Venables & Ripley 2002), the mclust 5.0 package (Scrucca *et al.* 2016) for model based clustering, StatMatch (D’Orazio 2015) and ade4 (Dray & Dufour 2007) for mantel tests, and all other analyses were performed using the base statistics module in R v.3.4.2 (R Core Team 2017).

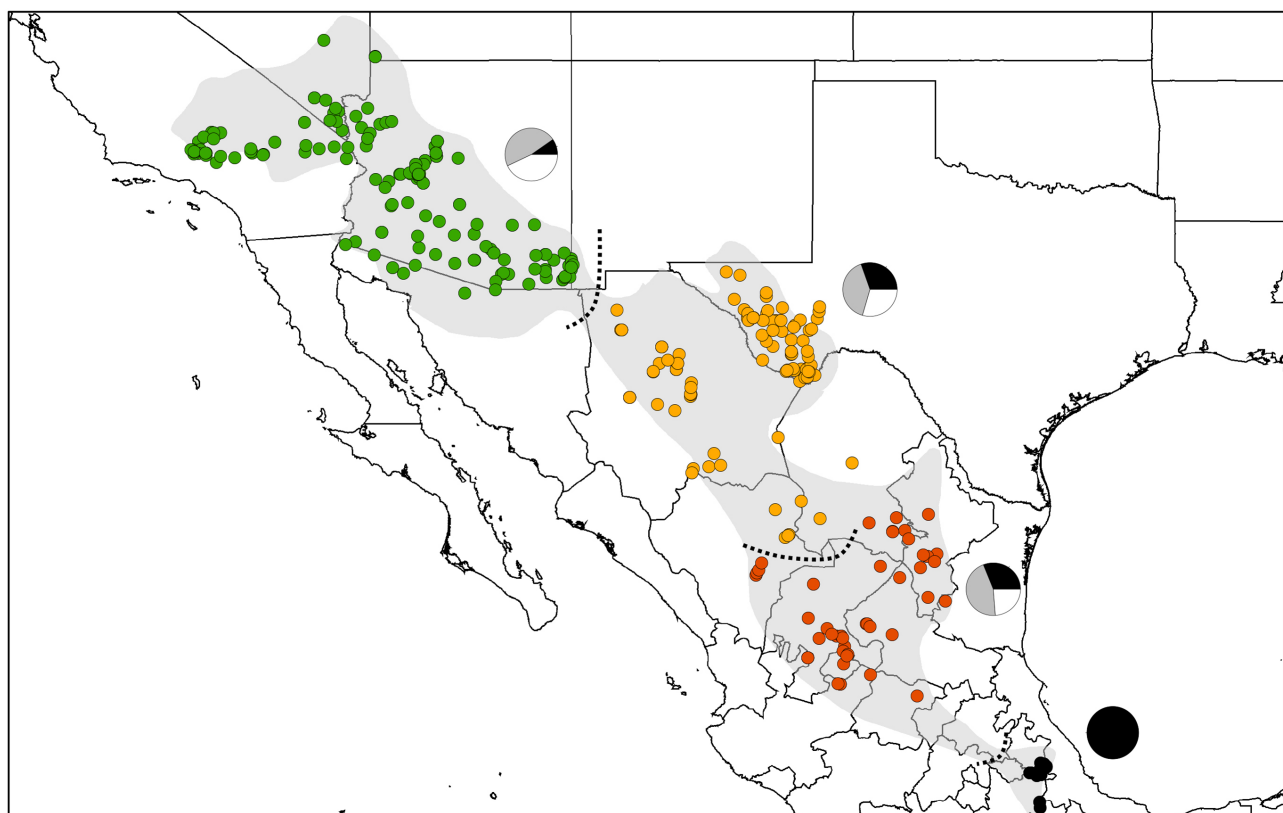


FIGURE 3. Geographic distribution of *Crotalus scutulatus*, with localities of specimens examined indicated by green symbols (Mohave-Sonoran lineage), yellow symbols (Chihuahuan lineage), orange symbols (Central Plateau lineage), and black symbols (*C. s. salvini* lineage). Pie-charts indicate relative frequencies of specimens with pale blotch borders absent (black), pale blotch borders indistinct (grey), and pale blotch borders distinct (white) for each genetic lineage.

Results

Summary data demonstrated extensive overlap of ranges for most quantitative characters across genetic lineages of *Crotalus scutulatus*, with a weak trend for lower mean or modal values for meristic traits in *C. s. salvini* (Table 1). Frequencies in condition of dorsal blotch borders varied significantly among lineages ($X^2 = 43.602$, $df = 6$, $p < 0.0001$), with the highest frequency of distinct pale blotch borders in the Mohave-Sonoran lineage, and a gradual decrease in frequency toward the south, with specimens assigned to *C. s. salvini* having 100% frequency of pale borders absent (Fig. 3). With respect to PCA, the first five axes collectively explained 74% of the total variance in our dataset, and were retained for further analysis. A scatterplot of the first three PC axes showed relatively strong phenotypic cohesion across all *C. scutulatus* samples, with visible differences in dispersion of specimens assigned to each lineage, but without clear distinction among lineages (Fig. 4A). Moreover, a scatterplot of the first three ca-

nonical axes from LDA demonstrated considerably more separation among specimens assigned to genetic lineages, but likewise did not separate lineages into discrete subgroups (Fig. 4B). Overall accuracy of LDA assignment of individuals to genetic lineages was 88.9%, and average posterior probabilities of assignment of individuals was 0.90, 0.85, 0.74, and 0.82 to Mohave-Sonoran, Chihuahuan, Central Plateau, and *C. s. salvini* lineages, respectively. Most misidentifications from LDA were from specimens assigned to geographically adjacent genetic lineages, and the relatively low posterior probability of assignment of individuals to the Central Plateau lineage reflected a moderate frequency of misidentification of specimens between the Central Plateau and Chihuahuan lineages. As a final assessment of phenotypic cohesion, our model-based clustering analysis of scores from the first five PC axes inferred only one inclusive cluster under the diagonal multivariate normal model, which had the lowest BIC value.

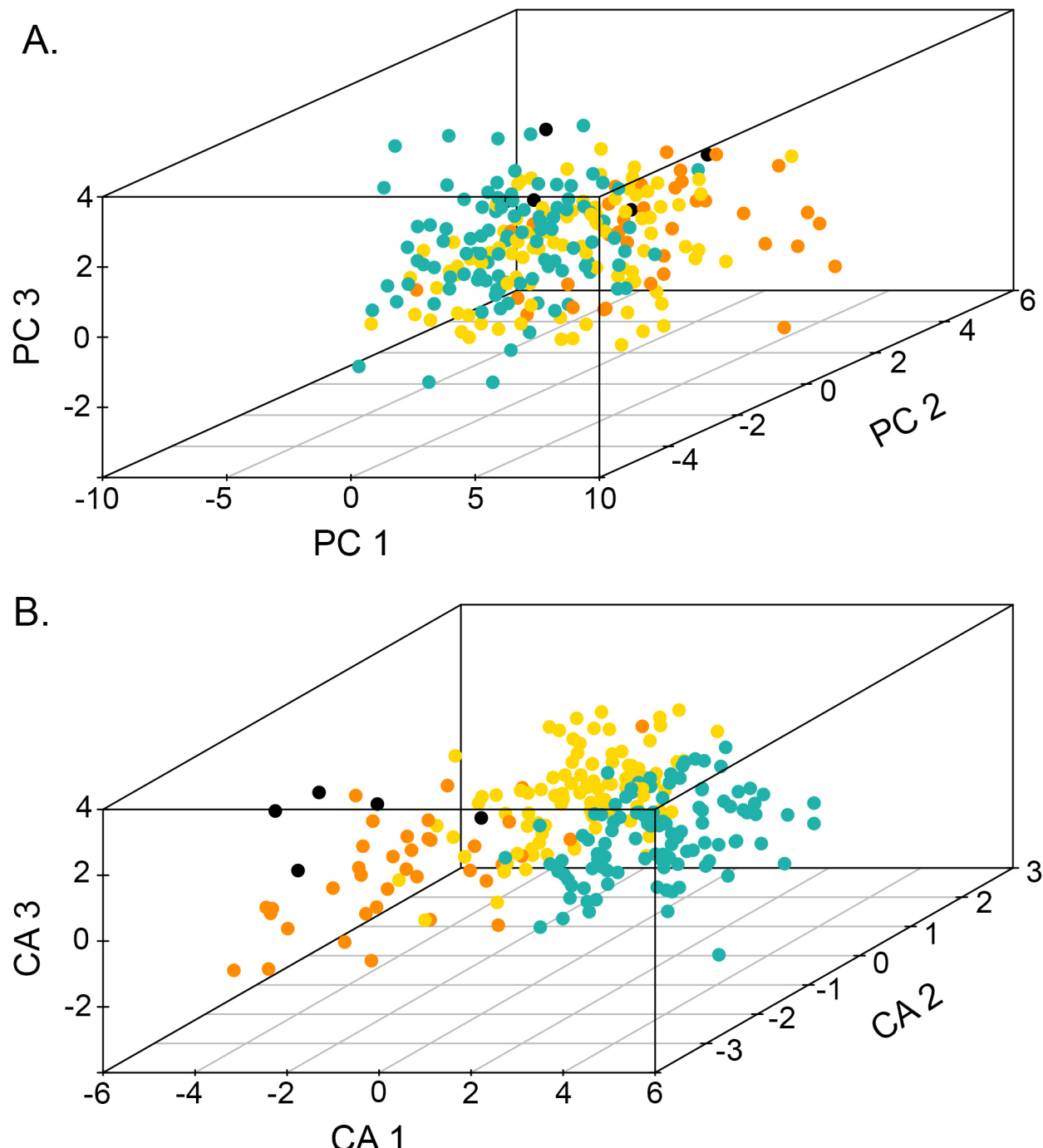


FIGURE 4. Scatterplots of factor scores from the first three principal component (PC) axes (A) and canonical scores from the first three canonical axes of a linear discriminant analysis (B) of multivariate phenotypic data from *Crotalus scutulatus* specimens. Symbol colors represent Mohave-Sonoran (green), Chihuahuan (yellow), Central Plateau (orange), and *Crotalus scutulatus salvini* (black) genetic lineages.

TABLE 1. Selected phenotypic characters for the genetic lineages of *Crotalus scutulatus*. For meristic characters, range is followed by mode, except for *C. s. salvini* due to small sample size or where there are multiple modal values, we presented the median (shown in bold). For snout vent length (SVL), range in mm is followed by the average. Values for males are shown above those for females.

Characters	<i>C. scutulatus</i> Mohave-Sonoran <i>n</i> = 167	<i>C. scutulatus</i> Chihuahuan <i>n</i> = 114	<i>C. scutulatus</i> Central Mexican Plateau <i>n</i> = 49	<i>C. scutulatus salvini</i> <i>n</i> = 17
Prefrontals	4–20 (8) 5–16 (9,11)	5–13 (6,8) 5–14 (8)	6–12 (6) 5–11 (6)	5–7 (6) 6–7 (6)
Interrictals	18–30 (26) 21–28 (25)	18–28 (24) 20–26 (23)	20–25 (22) 19–25 (24)	18–23 (21) 19–21 (20)
Supralabials	12–17 (15) 13–16 (15)	13–17 (15) 13–18 (15)	12–17 (14) 12–16 (14)	12–15 (13.5) 12–15 (13)
Infralabials	13–19 (16) 14–17 (15)	14–18 (16) 14–18 (16)	14–17 (15) 13–17 (15)	14–16 (14.5) 13–16 (14.5)
Ventrals	169–189 (176) 175–190 (184)	164–181 (173) 167–183 (177)	162–176 (165) 166–182 (168)	164–180 (169) 168–182 (177)
Subcaudals	19–32 (25) 14–24 (19)	16–29 (25) 15–25 (18)	13–26 (20) 11–21 (17)	16–28 (24) 16–21 (17)
Rattle fringe	10–13 (12) 10–14 (11)	9–14 (12) 9–13 (12)	10–13 (12) 10–14 (12)	10–14 (12) 11–14 (12)
Dorsal scale rows	23–28 (25) 22–28 (25)	24–28 (25) 24–27 (25)	25–28 (25) 24–29 (25)	22–30 (25) 24–26 (25)
Dorsal body blotches	27–43 (37) 32–42 (36)	27–43 (36) 31–47 (36)	25–39 (37) 30–42 (33)	28–33 (30) 29–35 (33)
Tail bands	3–8 (5) 2–6 (4)	2–6 (4) 2–6 (3)	2–6 (4) 2–5 (2,3)	3–7 (5) 3–4 (3)
SVL	478–1066 (752) 478–926 (702)	442–997 (722) 322–853 (616)	370–929 (624) 442–808 (610)	645–1067 (761) 470–833 (757)

Principal component axis 1 (42.1% of variance explained) reflected correlated variation in morphometric traits, for which all factor loadings weighted negatively, along with meristic traits SubC, Irect, and TB (Fig. 5; see Appendix 2 for character abbreviations). By contrast, PC 2 (11.5% of variance explained) reflected correlated variation in primarily meristic traits, with high values negatively correlated with this axis (Fig 5). Four characters, HL, HW, MBL, and MBI were positively correlated with PC2 with moderately high factor loadings, and this axis also showed the greatest differences in mean values across genetic lineages as indicated by the highest *f*-value from ANOVA comparisons (Fig. 5; Table 2). The PC 3 (7.7% of variance explained) reflected aspects of sexual dimorphism that were consistent across genetic lineages, with CL, SubC, DBB, and TB positively correlated, and DSR, Slab, Ilab, and Irect, inversely correlated with this axis, respectively. By contrast, PC 4 (7.2% of variance explained) reflected sexually dimorphic traits that varied across genetic lineages (lineage and sex interaction), with BL, Vent, PreF, and DBB positively correlated, and CL, SubC, Slab, Ilab, and TB negatively correlated along this axis. Finally, variation in PC 5 (5% of variance explained) did not reflect a clear pattern with respect to phenotypic variation across lineages or between sexes, and we interpret this axis to represent primarily “noise” variation consistent across both lineages and sexes.

Two-way ANOVAs with lineage and sex as factors inferred a general pattern of significant differences between lineage and sexes in mean PC factor scores, with minimal interaction effects between factors (Fig. 5; Table 2). Least squares linear regression analyses of the first five PC axes against latitude and longitude indicated a general pattern of slopes that differed significantly from zero (Table 3). With the exception of PC 2, latitude and longitude generally explained little variation in PC factor scores (i.e., adjusted R^2 -values < 0.2); however, PC 2 demonstrated a relatively strong relationship between factor scores and latitude ($R^2 = 0.43$) as well as between factor scores and longitude (R^2

= 0.31; Fig. 6). Because PC 4 reflected variation among sexually dimorphic traits and lineages simultaneously, this axis also had relatively high R^2 -values for the effects of latitude and longitude (Table 3). Mantel tests also revealed an overall morphological pattern consistent with “isolation-by-distance” ($R = 0.17, p < 0.0001$). In our analysis of relative head length among lineages, we did not reject the null hypothesis of equal slopes ($p = 0.21$), and also found significant differences in relative head size (i.e., intercepts of HL on BL) among genetic lineages of *C. scutulatus*, with specimens of *C. s. salvini* and the Central Plateau lineages showing greater relative head size than specimens from the northern two lineages ($F = 2556.87, df = 1,3, p < 0.0001$; Fig. 7).

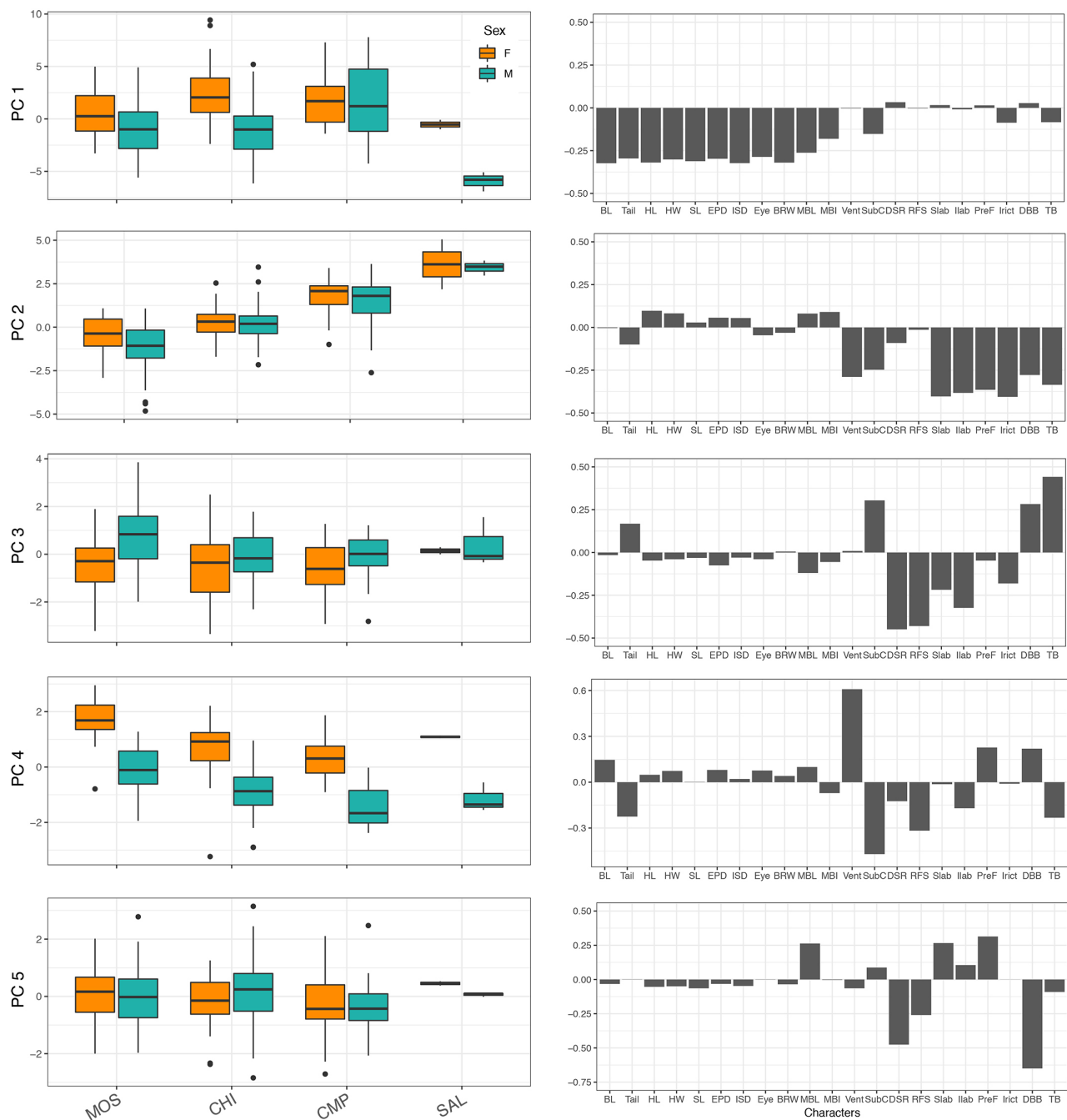


FIGURE 5. Boxplots of factor scores from the first five principal component (PC) axes for each lineage separated by sex (left panel), and PC factor loadings for each character on respective PC axes (right panel). Lineage abbreviations are as follows: MOS (Mohave-Sonoran), CHI (Chihuahuan), CMP (Central Plateau), SAL (*Crotalus scutulatus salvini*). Character abbreviations are provided in Appendix 2.

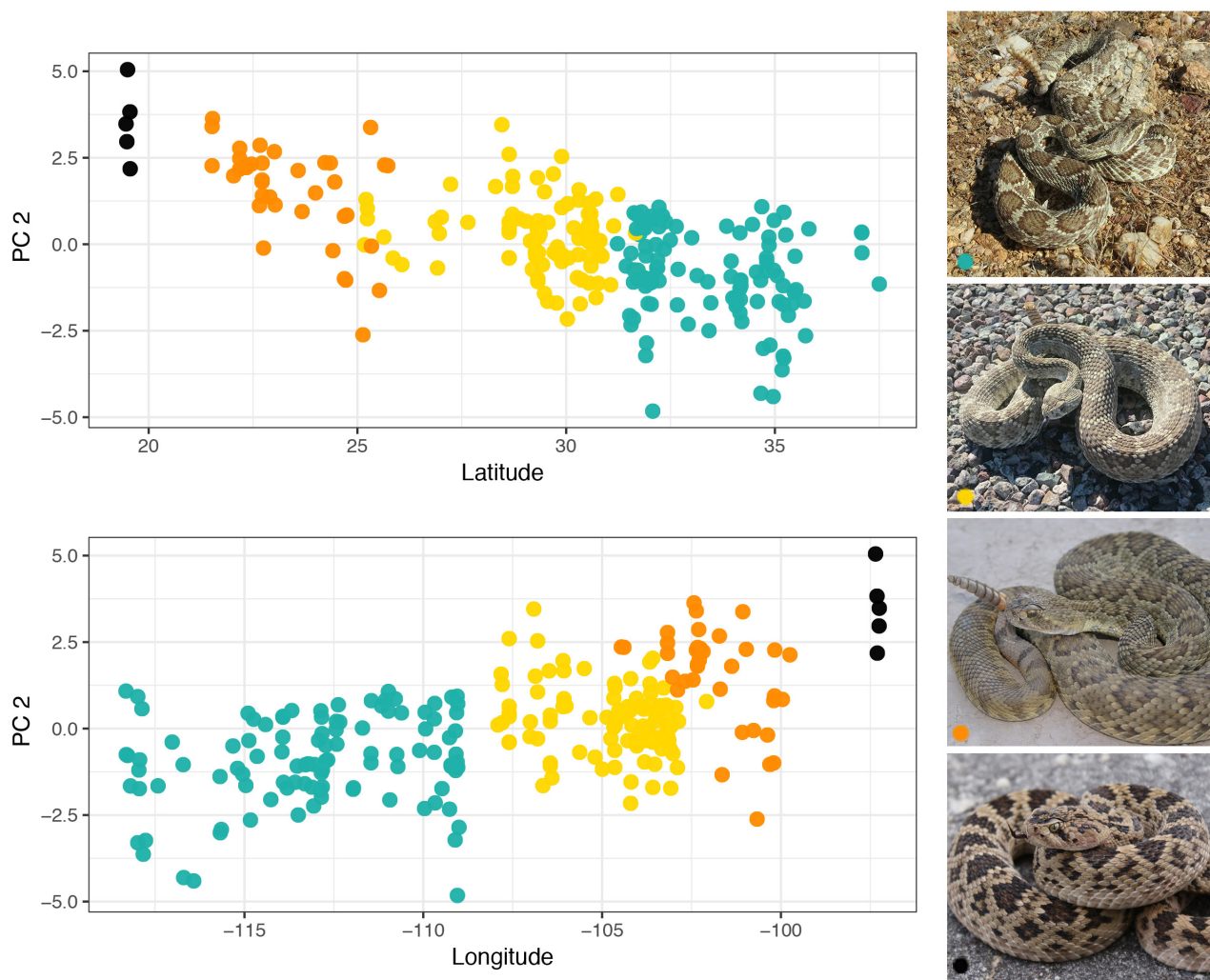


FIGURE 6. Principal component (PC) factor scores for axis 2 regressed on latitude and longitude, showing clinal variation of phenotypes within *Crotalus scutulatus* (left panel), and photographs in life of *C. scutulatus* individuals representative of each genetic lineage (right panel). Symbol colors represent Mohave-Sonoran (green), Chihuahuan (yellow), Central Plateau (orange), and *C. s. salvini* (black) lineages. Photo credits from top to bottom: JMM (south of Wellton, Yuma Co., Arizona), JMM (west of Davis Mountains, Jeff Davis Co., Texas), Michael Price (Huizache, San Luis Potosí, Mexico), and Carlos Hernández-Jiménez (Jalapasco Tepayahualco, Puebla, Mexico).

TABLE 2. Two-way ANOVA results with Lineage and Sex as factors and factor scores from the first five PC axes as the dependent variable.

Dependent Variable	Lineage			Sex			Lineage:Sex		
	DF	f-value	p-value	DF	f-value	p-value	DF	f-value	p-value
PC 1	3	10.922	< 0.0001	1	35.240	< 0.0001	3	3.616	0.0139
PC 2	3	57.060	< 0.0001	1	7.212	0.0078	3	0.972	0.4068
PC 3	3	7.411	< 0.0001	1	25.362	< 0.0001	3	2.528	0.0581
PC 4	3	27.850	< 0.0001	1	244.493	< 0.0001	3	0.592	0.621
PC 5	3	1.821	0.144	1	0.581	0.447	3	0.654	0.581

TABLE 3. Least squares linear regressions of factor scores from the first five principal component (PC) axes against latitude and longitude.

Source		B	SE B	t-value	p-value	Adjusted R ²
PC 1	Latitude	-0.161	0.046	-3.499	0.0006	0.044
	Longitude	0.088	0.036	2.419	0.0163	0.020
PC 2	Latitude	-0.251	0.019	-13.44	< 0.0001	0.426
	Longitude	0.165	0.016	10.35	< 0.0001	0.305
PC 3	Latitude	0.048	0.020	2.423	0.0161	0.020
	Longitude	-0.054	0.015	-3.498	0.0006	0.044
PC 4	Latitude	0.091	0.019	4.911	< 0.0001	0.087
	Longitude	-0.097	0.014	-7.002	< 0.0001	0.166
PC 5	Latitude	0.027	0.016	1.676	0.095	0.007
	Longitude	-0.019	0.013	-1.479	0.140	0.005

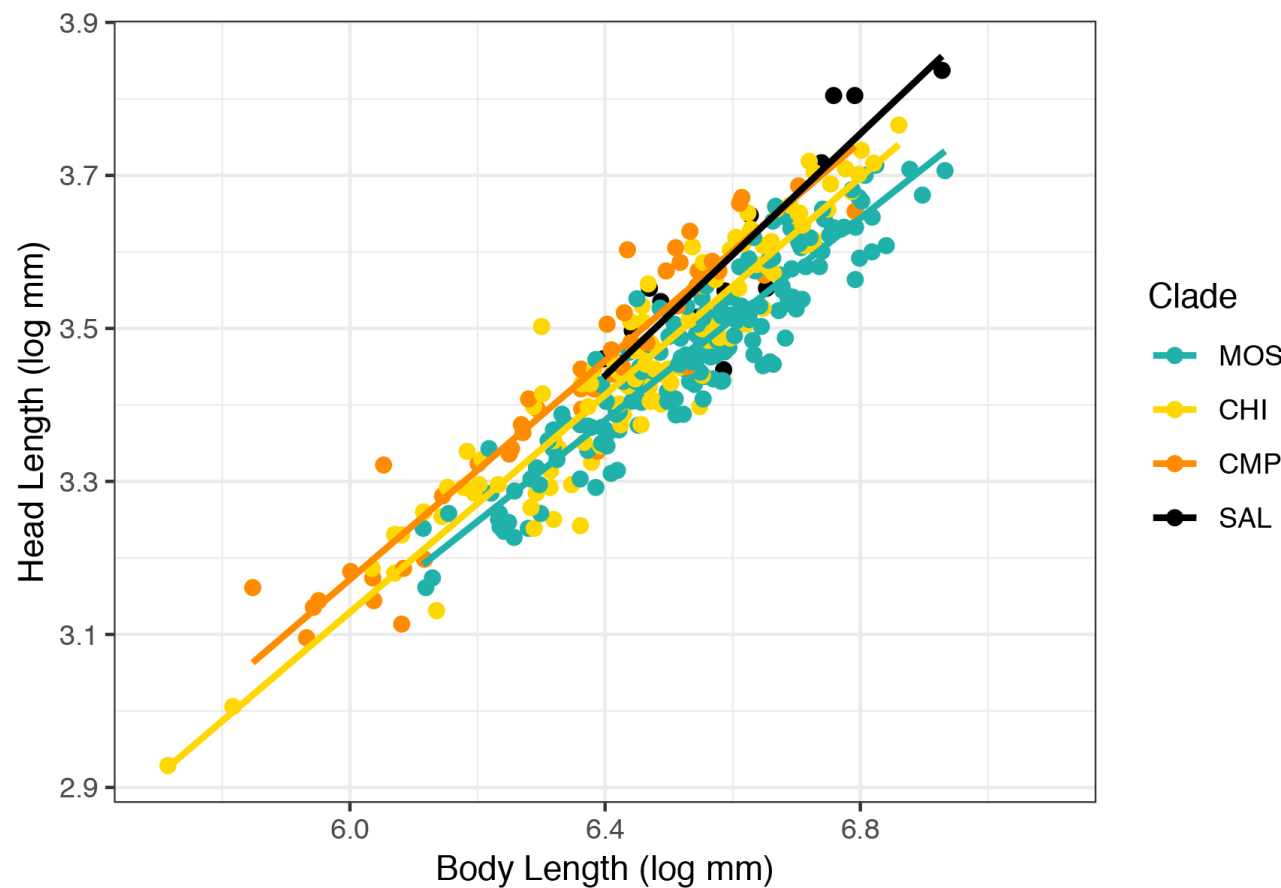


FIGURE 7. Scaling relationship of head length (log mm) and body length (log mm) for each genetic lineage of *Crotalus scutulatus*. Lineage abbreviations are as follows: MOS (Mohave-Sonoran), CHI (Chihuahuan), CMP (Central Plateau), SAL (*Crotalus scutulatus salvini*).

Discussion

Our results demonstrate that *Crotalus scutulatus* exhibits variation in morphology that follows a cline along the major axis of its expansive geographic distribution. Relative to southeastern specimens, Mohave rattlesnakes from the northwestern part of their range had relatively high values for CL, Vent, SubC, DSR, Slab, Ilab, PreF, Ircit, DBB, and TB, and relatively low values for HL, HW, MBL, and MBI (Figs. 5–6). Although this finding is consistent with early interpretations of variation in *C. scutulatus* (e.g., Klauber 1930; Gloyd 1940), no previous studies have evaluated phenotypic variation across the distribution of this taxon in an explicit statistical and geographical context. The major genetic lineages differed in mean values of multiple traits with respect to PC factor scores (Table 2). Overall

phenotypic variation, however, was continuous and lacked any discrete gaps or shifts in multivariate distributions across genetic lineage boundaries. Importantly, the results from model-based clustering indicate that all *C. scutulatus* sampled are included in a single cohesive phenotypic cluster that was diagonal multivariate normal.

Along with previously published genetic data, our phenotypic dataset provides additional insight into patterns of variation and divergence relevant to species delimitation in *C. scutulatus*. Hypothesis A posits that each of the four genetic lineages inferred by Schielf *et al.* (2018) should be elevated to species (Fig. 1). This hypothesis acknowledges past population fragmentation and divergence within an ancestral lineage that temporally coincides with Pleistocene glacial cycles, and emphasizes the signature of these demographic events in genetic data (Schielf *et al.* 2018). However, this hypothesis does not necessarily capture the complex demographic history and patterns of gene flow between genetic lineages, as demonstrated by evaluations of allele frequency spectra between pairwise *C. scutulatus* lineages, which indicate secondary contact or migration at all boundaries within major genetic lineages. In the present study, phenotypic data are consistent with expectations of past and/or ongoing gene flow between all adjacent *C. scutulatus* lineages, and in terms of morphological distinction or diagnosis, distinguishing species within a four-species model would be untenable.

Hypothesis B, or the “expanded *salvini*” concept, posits that species boundaries coincide with the deepest genetic lineage divergence, whereby *C. scutulatus* would consist of Mohave-Sonoran and Chihuahuan populations, and *C. salvini* would comprise all populations from the Central Plateau southward (Fig. 1). One of the merits of this hypothesis is that Central Plateau and *C. s. salvini* populations together form a clade in phylogenetic inferences (Schielf *et al.* 2018). However, Schielf *et al.* (2018) also inferred relatively low levels of nuclear allelic differentiation between Central Plateau and Chihuahuan lineages, which could indicate relatively high levels of gene flow between these groups, or could be an artifact of the large geographic area without molecular samples between the Mohave-Sonoran and Chihuahuan groups. Morphological differentiation across the Central Plateau and Chihuahuan clade boundary was also minimal, and the low average posterior probability of classification of Central Plateau specimens primarily was due to high misclassification of specimens between these lineages. Hypothesis C is similar to Hypothesis B in that it is consistent with a combined interpretation of mtDNA and nuclear coalescent species trees, but also suffers the same drawbacks to Hypothesis B in that it is not supported by phenotypic data and shows both low nuclear differentiation and a relatively strong signal for historical gene flow between Chihuahuan and Central Plateau populations. The “expanded *salvini*” concepts are somewhat supported by the observation that Central Plateau and *Crotalus s. salvini* populations tend to have proportionately larger heads than do snakes from the northern lineages. However, relative HL contributes to the overall pattern of clinal variation in *C. scutulatus* phenotypes (Figs. 5–6), and shows high variation within and among populations (Fig. 7).

Hypothesis D is based partially on the legacy taxonomy of the past century, when both subspecies of *C. scutulatus* were formalized based on putative phenotypic distinctions (Klauber 1930, 1972; Gloyd 1940; Fig. 1). Our results are in general agreement with phenotypic data presented by Gloyd (1940) and Klauber (1930, 1972), but these early assessments were based largely on comparisons of specimens from the extreme northern and southern parts of the distribution of *C. scutulatus*, with relatively few specimens available to confirm clinal variation from the large gap across central Mexico. Individuals from the extreme northwestern and southeastern parts of *C. scutulatus* distribution are considerably different from each other in overall coloration and pattern (Fig. 6), with *C. s. salvini* having border-free chocolate dorsal blotches against a buff to pink background color, and often with striking jade-colored irises. However, our more expansive dataset including numerous specimens from central Mexico confirms the overall pattern of clinal variation predicted by Gloyd (1940), and further diminishes the diagnosability of *C. s. salvini* as a species distinct from *C. s. scutulatus*. In addition to a gradual increase in values of most meristic traits from south to north, we also note that the condition of distinct pale blotch borders increases in frequency from south to north across the distribution of *C. scutulatus*, rather than being diagnostic of *C. s. scutulatus* (Fig. 3). Although *C. s. salvini* constitutes a distinct lineage based on mitochondrial gene tree and nuclear coalescent species tree analyses, considering *C. s. salvini* an independent lineage/species from the Central Plateau lineage had the lowest support of all four lineages tested based on nuclear data in Schielf *et al.* (2018). Based on a large nuclear SNP dataset, the demographic history at the boundary between *C. s. scutulatus* and *C. s. salvini* was inferred as “divergence with ancestral symmetrical migration” (Schielf *et al.* 2018), suggesting pervasive gene flow or very recent divergence. However, as noted by Schielf *et al.* (2018), these mitochondrial/nuclear discrepancies do not preclude the possibility that *C. s. salvini* could represent a peripheral isolate population in the early process of speciation that has yet to complete lineage sorting. Unfortunately, there is a dearth of material available from the southern Central Plateau

region (e.g., Queretaro, Hidalgo) despite recent field efforts, and it is unclear if this reflects sampling bias or an actual recent distributional hiatus between *C. s. scutulatus* and *C. s. salvini*.

Collectively, phenotypic data in context with previously published molecular studies suggest that Hypothesis E, the single species model, is the most parsimonious delimitation of species within *C. scutulatus* (Fig. 1). As expected, phenotypic data were generally congruent with nuclear data and support the notion that isolated geographic lineages of *C. scutulatus* currently, or until recently, have experienced secondary contact and renewed gene flow. Furthermore, our finding of continuous clinal variation within *C. scutulatus* emphasizes the importance of morphological data in robust species delimitation, as broadly expanded genetic datasets are likely to reveal complex demographic scenarios that can obscure a straightforward delineation of lineages. In such contexts, morphological data can help identify pragmatic taxonomic solutions where genetic data alone do not provide a clear solution. The juxtaposition of morphological and genetic datasets within *C. scutulatus* illustrates an interesting case of a wide-ranging species that harbors substantial genetic diversity, and that has experienced a unique demographic history involving extensive gene flow between cryptic genetic lineages, which we conclude has likely influenced the observed pattern of clinal variation in morphology. This perception of *C. scutulatus* conforms to the general lineage concept of species as metapopulation lineages (de Queiroz 1998, 2007), and exemplifies how both fine-scale molecular data and phenotypic data can now delimit the boundaries of these (meta)populations within cohesive, widespread species.

Acknowledgements

We thank the following institutions for facilitating access to preserved materials: BMNH (J. Streicher), BYU (J. Sites Jr., S. Skidmore, A. Whiting), CAS (L. Scheinberg, J. Vindum, E. Ely), CNAR (G. Parra Olea, V. Reynosa Rosales), ENCB (G. Campillo García, D. Antonio Rangel, J. López Vidal), FMNH (A. Resetar), KU (R. Brown, R. Glor, L. Welton), MVZ (N. Stepanova, J. McGuire), MZFC (E. Pérez-Ramos), SDNHM (B. Hollingsworth, M. Stepek), TCWC (T. Hibbitts, L. Fitzgerald), TNHC (T. LaDuc, D. Cannatella), UAA (J. Sigala Rodríguez), UTA (C. Franklin, E. Smith), and all the generous people that assisted in the field or collected specimens. This work was supported by National Science Foundation (NSF) grant DEB-1655571 to TAC and SPM and UC MEXUS-CONACYT CN-11-548 grant to CLS, OF-V, LLS and SPM.

References

Baird, S.F. & Girard, C. (1853) *Catalogue of North American reptiles in the Museum of the Smithsonian Institution. Part I. Serpents*. GPO, Washington, D.C., 172 pp.
<https://doi.org/10.5962/bhl.title.5513>

Cadena, C.D., Zapata, F. & Jiménez, I. (2018) Issues and perspectives in species delimitation using phenotypic data: Atlantean evolution in Darwin's finches. *Systematic Biology*, 67 (2), 181–194.
<https://doi.org/10.1093/sysbio/syx071>

Campbell, J.A. & Lamar, W.W. (2004) *The Venomous Reptiles of the Western Hemisphere*. Cornell University Press, Ithaca, 870 pp.

Cardwell, M.D. (2016) Mohave rattlesnake, *Crotalus scutulatus* (Kennicott 1861). In: Schuett, G.W., Feldner, M.J., Smith, C.F. & Reiserer, R.S. (Eds.), *Rattlesnakes of Arizona. Vol. 1*. ECO Publishing, Rodeo, pp. 563–606.

Coyne, J.A. & Orr, H.A. (2004) *Speciation*. Sinauer Associates, Sunderland, 545 pp.

de Queiroz, K. (1998) The general lineage concept of species, species criteria, and the process of speciation: A conceptual unification and terminological recommendations. In: Howard, D.J. & Berlocher, S.H. (Eds.), *Endless Forms: Species and Speciation*. Oxford University Press, New York City, pp. 57–75.

de Queiroz, K. (2007) Species concept and species delimitation. *Systematic Biology*, 56 (6), 879–886.
<https://doi.org/10.1080/10635150701701083>

D’Orazio, M. (2015) Integration and imputation of survey data in R: the StatMatch package. *Romanian Statistical Review*, 2, 57–68.

Douglas, M.E., Douglas, M.R., Schuett, G.W. & Porras, L.W. (2006) Evolution of rattlesnakes (Viperidae; *Crotalus*) in the warm deserts of western North America shaped by Neogene vicariance and Quaternary climate change. *Molecular Ecology*, 15 (11), 3353–3374.
<https://doi.org/10.1111/j.1365-294X.2006.03007.x>

Dray, S. & Dufour, A. (2007) The ade4 package: Implementing the duality diagram for ecologists. *Journal of Statistical Software*, 22 (4), 1–20.

https://doi.org/10.18637/jss.v022.i04

Feder, J.L., Egan, S.P. & Nosil, P. (2012) The genomics of speciation-with-gene-flow. *Trends in Genetics*, 28 (7), 342–350.
<https://doi.org/10.1016/j.tig.2012.03.009>

Fisher, R.A. (1918) The correlation between relatives on the supposition of Mendelian inheritance. *Transactions of the Royal Society of Edinburgh*, 52, 399–433.
<https://doi.org/10.1017/S0080456800012163>

Fraley, C. & Raftery, A.E. (2007) Model-based methods of classification: using the mclust software in chemometrics. *Journal of Statistical Software*, 18 (6), 1–13.
<https://doi.org/10.18637/jss.v018.i06>

Gloyd, H.K. (1940) *The Rattlesnakes, Genera Sistrurus and Crotalus: A Study in Zoogeography and Evolution*. Chicago Academy of Sciences, Chicago, 266 pp.
<https://doi.org/10.2307/1437993>

Gutberlet, R.L. Jr. & Harvey, M.B. (2002) Phylogenetic relationships of new world pitvipers as inferred from anatomical evidence. In: Schuett, G.W., Höggren, M., Douglas, M.E. & Greene, H.W. (Eds.), *Biology of the Vipers*. Eagle Mountain Publishing, LC, Eagle Mountain, pp. 51–68.

Kennicott, R. (1861) On three new forms of rattlesnakes. *Proceedings of the Academy of Natural Sciences of Philadelphia* 13, 204–208.

Klauber, L.M. (1930) New and renamed subspecies of *Crotalus confluens* Say, with remarks on related species. *Transactions of the San Diego Society of Natural History*, 6, 95–144.
<https://doi.org/10.5962/bhl.part.11694>

Klauber, L.M. (1972) *Rattlesnakes: Their habits, Life Histories, and Influence on Mankind*. 2 Vols. University of California Press, Berkeley, 1533 pp.

Mantooth, S.J., Hafner, D.J., Bryson, R.W. Jr. & Riddle, B.R. (2013) Phylogenetic diversification of antelope squirrels (*Ammospermophilus*) across North American deserts. *Biological Journal of the Linnean Society*, 109, 949–967.
<https://doi.org/10.1111/bij.12084>

Meik, J.M., Streicher, J.W., Lawing, A.M., Flores-Villela, O. & Fujita, M.K. (2015) Limitations of climatic data for inferring species boundaries: insights from speckled rattlesnakes. *PLoS ONE*, 1, e0131435.
<https://doi.org/10.1371/journal.pone.0131435>

Meik, J.M., Schaack, S., Flores-Villela, O. & Streicher, J.W. (2018) Integrative taxonomy at the nexus of population divergence and speciation in insular speckled rattlesnakes. *Journal of Natural History*, 52 (13–16), 989–1016.
<https://doi.org/10.1080/00222933.2018.1429689>

Myers, E.A., Hickerson, M.J. & Burbrink, F.T. (2016) Asynchronous diversification of snakes in the North American warm deserts. *Journal of Biogeography*, 44, 461–474.
<https://doi.org/10.1111/jbi.12873>

Nosil, P. & Feder, J.L. (2012) Genomic divergence during speciation: causes and consequences. *Philosophical Transactions of the Royal Society B*, 367, 332–342.
<https://doi.org/10.1098/rstb.2011.0263>

R Core Team. (2017) R: A language and environment for statistical computing. R Foundation for Statistical Computing, Vienna. Available from: <https://www.R-project.org/> (accessed 4 June 2019)

Rafinesque, C.S. (1818) Natural history of the *Scytalus Cupreus*, or copper-head snake. *American Journal of Science*, 1 (1), 84–88.

Riddle, B.R. & Hafner, D.J. (2006) A step-wise approach to integrating phylogeographic and phylogenetic biogeographic perspectives on the history of a core North American warm deserts biota. *Journal of Arid Environments*, 66 (3), 435–461.
<https://doi.org/10.1016/j.jaridenv.2006.01.014>

Sabaj, M.H. (2016) Standard symbolic codes for institutional resource collections in herpetology and ichthyology: an online reference. Version 6.5. American Society of Ichthyologists and Herpetologists. Available from: <http://www.asih.org/> (accessed 3 June 2019)

Schield, D.R., Card, D.C., Adams, R.H., Jezkova, T., Reyes-Velasco, J., Proctor, F.N., Spencer, C.L., Herrmann, H.W., Mackessy, S.P. & Castoe, T.A. (2015) Incipient speciation with biased gene flow between two lineages of the Western Diamondback Rattlesnake (*Crotalus atrox*). *Molecular Phylogenetics and Evolution*, 83, 213–223.
<https://doi.org/10.1016/j.ympev.2014.12.006>

Schield, D.R., Adams, R.H., Card, D.C., Corbin, A.B., Jezkova, T., Hales, N.R., Meik, J.M., Perry, B.W., Spencer, C.L., Smith, L.L., García, G.C., Bouzid, N.M., Strickland, J.L., Parkinson, C.L., Borja, M., Castañeda-Gaytán, G., Bryson, R.W.Jr., Flores-Villela, O.A., Mackessy, S.P. & Castoe, T.A. (2018) Cryptic genetic diversity, population structure, and gene flow in the Mojave rattlesnake (*Crotalus scutulatus*). *Molecular Phylogenetics and Evolution*, 127, 669–681.
<https://doi.org/10.1016/j.ympev.2018.06.013>

Schield, D.R., Perry, B.W., Adams, R.H., Card, D.C., Jezkova, T., Pasquesi, G.I.M., Nikolakis, Z.L., Row, K., Meik, J.M., Smith, C.F., Mackessy, S.P. & Castoe, T.A. (2019) Allopatric divergence and secondary contact with gene flow – a recurring theme in rattlesnake speciation. *Biological Journal of the Linnean Society*, 128, 149–169.
<https://doi.org/10.1093/biolinnean/blz077>

Scrucca, L., Fop, M., Murphy, T.B. & Raftery, A.E. (2016) mClust 5: clustering, classification and density estimation using

Gaussian finite mixture models. *The R Journal*, 8, 205–233.
<https://doi.org/10.32614/RJ-2016-021>

Strickland, J.L., Mason, A.J., Rokyta, D.R. & Parkinson, C.L. (2018a) Phenotypic variation in Mojave rattlesnake (*Crotalus scutulatus*) venom is driven by four toxin families. *Toxins*, 10 (4), 1–23.
<https://doi.org/10.3390/toxins10040135>

Strickland, J.L., Smith, C.F., Mason, A.J., Schield, D.R., Borja, M., Castañeda-Gaytán, G., Spencer, C.L., Smith, L.L., Trápanga, A., Bouzid, N.M., Campillo-García, G., Flores-Villela, O.A., Antonio-Rangel, D., Mackessy, S.P., Castoe, T.A., Rokyta, D.R. & Parkinson, C.L. (2018b) Evidence for divergent patterns of local selection driving venom variation in Mojave Rattlesnakes (*Crotalus scutulatus*). *Scientific Reports*, 8, 1–15.
<https://doi.org/10.1038/s41598-018-35810-9>

Sullivan, J., Demboski, J.R., Bell, K.C., Hird, S., Sarver, B., Reid, N. & Good, J.M. (2014) Divergence with gene flow within the recent chipmunk radiation (*Tamias*). *Heredity*, 113 (3), 185–194.
<https://doi.org/10.1038/hdy.2014.27>

Templeton, A.R. (2006) *Population Genetics and Microevolutionary Theory*. John Wiley and Sons, Hoboken, 718 pp.
<https://doi.org/10.1002/0470047356>

Venables, W.N. & Ripley, B.D. (2002) *Modern Applied Statistics with S 4th edition*. Springer, New York, 498 pp.
<https://doi.org/10.1007/978-0-387-21706-2>

Wood, D.A., Meik, J.M., Holycross, A.T., Fisher, R.N. & Vandergast, A.G. (2008) Molecular and phenotypic diversity in *Chionactis occipitalis* (Western shovel-nosed snake), with emphasis on the status of *C. o. klauberi* (Tucson shovel-nosed snake). *Conservation Genetics*, 9 (6), 1489–1507.
<https://doi.org/10.1007/s10592-007-9482-0>

Wood, D.A., Vandergast, A.G., Barr, K.R., Inman, R.D., Esque, T.C., Nussear, K.E. & Fisher, R.N. (2013) Comparative phylogeography reveals deep lineages and regional evolutionary hotspots in the Mojave and Sonoran Deserts. *Diversity and Distributions*, 19, 722–737.
<https://doi.org/10.1111/ddi.12022>

Wu, C.I. & Ting, C.T. (2004) Genes and speciation. *Nature*, 5, 114–122.
<https://doi.org/10.1038/nrg1269>

Zancolli, G., Calvete, J.J., Cardwell, M.D., Greene, H.W., Hayes, W.K., Hegarty, M.J., Herrmann, H.W., Holycross, A.T., Lannutti, D.I., Mulley, J.F., Sanz, L., Travis, Z.D., Whorley, J.R., Wüster, C.E. & Wüster, W. (2019) When one phenotype is not enough: divergent evolutionary trajectories govern venom variation in a widespread rattlesnake species. *Proceedings of the Royal Society B: Biological Sciences*, 286, 20182735.
<https://doi.org/10.1098/rspb.2018.2735>

APPENDIX 1. Specimens examined

***Crotalus scutulatus*.** MEXICO ($n = 121$): AGUASCALENTES: CAS 87400; ENCB 13451; MVZ 275536; TCWC 38569; UTA 18360. CHIHUAHUA: BYU 13871–72, 15313–14, 15321, 15344, 15349–51, 15678, 17108, 17113, 19133, 21717; KU 35093; 45339–45, 62865, 75643; MVZ 68913, 71036–37, 71040, 71050, 73115, 73117, 73123, 84509; TNHC 101199, 105694; UTA 4554, 12587, 17932, 58939. COAHUILA: CAS–SU 27236; FMNH 44317; KU 39952; TCWC 38991, 54241; TNHC 29870, 33887, 112044. DURANGO: BYU 40051–52; CAS 120880; FMNH 103000; ENCB 16074; KU 39955; MVZ 143532; MZFC 17996; TCWC 43327; TNHC 29761. GUANAJUATO: MVZ 275539. JALISCO: KU 95973–75, 102987, 102990–92. NUEVO LEON: KU 187318; SDNHM 57004; TCWC 36012, 54242, 60785–86; TNHC 29866, 29871, 112041; UTA 4595. PUEBLA: CNAR 6970; FMNH 106061; ENCB 1116; MVZ 275548, 275552 (MZFC 26289); MZFC 4305, 25208. SAN LUIS POTOSI: CAS 169831; ENCB 108, 8151; MVZ 275546–47. SONORA: CNAR 48, 6978; MVZ 81284–85; SDNHM 2327, 37635, 49711. TAMAULIPAS: SDNHM 6573. TLAXCALA: CNAR 6218. VERACRUZ: BYU 42717, 42726; KU 23750, 26688; MVZ 275543–45; MZFC 2008, 25166. ZACATECAS: CAS 96077; KU 29489, 29490, 39956, 45000; MVZ 143533, 275549–50; SDNHM 49713; TCWC 56448; UTA 2715.

UNITED STATES ($n = 226$): ARIZONA: Cochise Co.: BYU 5406; FMNH 207793; MVZ 209102, 209105, 215712, 226243, 229828, 229829, 229831, 229836; TCWC 85929; TNHC 60138, 105691, 105692, 112040; UTA 10024, 10025, 35042, 38798, 38800. Coconino Co.: SDNHM 2105–08, 2130–32. Graham Co.: CAS 170506; SDNHM 40618. La Paz Co.: MVZ 233686, 233690–93. Maricopa Co.: CAS 65089, 65699; MVZ 129357, 129359, 233684; SDNHM 25556–57, TNHC 58831. Mohave Co.: MVZ 275561–62, 277717; SDNHM 867, 1145, 1820, 3484, 17305, 29702, 31779, 39023, 41584. Pima Co.: CAS 192717; FMNH 207794; MVZ 196873, 233673; SDNHM 2766, 23235; UTA 14465, 32336–37, 32343. Pinal Co.: CAS 192742; SDNHM 2767, 17074. Santa Cruz Co.: CAS 80762; MVZ 76672; SDNHM 17948, 20926. Yavapai Co.: CAS 63881–83, 65111, 65693, 156178; MVZ 70299, 97145–46, 233696–97; SDNHM 2025, 2044–46, 2080, 2122–24, 2182, 3039, 3463, 5449, 5566–67, 9302, 17628–30. YUMA Co.: SDNHM 2684, 2708; UTA 45169. CALIFORNIA: Kern Co.: CAS 91629; KU 62904; MVZ

31734, 137600, 193456–58, 193460, 233699. Los Angeles Co.: BYU 42690, 42708; MVZ 11430, 275565; SDNHM 838, 865, 1656–57, 2409, 2810, 20118, 33688, 37967, 43609. San Bernardino Co.: BMNH 1987.1231; BYU 41724; CAS 228094, 250115, 259911; KU 31352; MVZ 18034, 26666, 176158, 193464, 233782–83; SDNHM 2605, 10549. NEVADA: Clark Co.: BYU 52748, 62939, 63056; CAS 156168; MVZ 275567, 277732, 277738–39; SDNHM 4396. Lincoln Co.: MVZ 14304. NEW MEXICO: Hidalgo Co.: TCWC 56318; TNHC 104537; UTA 51371, 53919–20, 53924–25. TEXAS: Brewster Co.: KU 13782, 61326, 177079–82, 319075, 336523, 336525, 341047; TCWC 4748, 16148, 16150, 27534–35, 29404, 33377, 36356–57, 36906, 40098, 40100, 64342, 64556, 86017, 88019, 103248; TNHC 33886, 85217, 89444, 92383; UTA 53729. Culberson Co.: TCWC 33376, 77638; UTA 44383. Hudspeth Co.: TCWC 18394; TNHC 87883. Jeff Davis Co.: CAS 170519; TCWC 72829, 84534, 91848; TNHC 66531, 66539, 66881–82, 87880, 89782, 89786, 89855, 89857, 97400–01; UTA 3901, 53945, 61674. Pecos Co.: SDNHM 916; TNHC 89831; UTA 44376. Presidio Co.: KU 336524; TCWC 27533, 80604, 90727; TNHC 66436, 66530, 66532–33. UTAH: Washington Co.: BYU 35963, 42699, 42849.

APPENDIX 2. Morphological characters

1. Body length, measured in mm (BL);
2. Tail length, measured in mm (CL);
3. Head length measured to 0.1 mm from face of the rostral to the angle of the quadrate and mandible (HL);
4. Head width measured to 0.1 mm at widest point (HW);
5. Snout length measured to 0.1 mm from anterior edge of the eye to the center of the rostral plate (SL);
6. Eye-to-pit distance measured to 0.1 mm from the shortest distance between anterior edge of eye to posterior edge of pit organ (EPD);
7. Intersupraocular distance measured to 0.1 mm from the lateral edge of each supraocular scale (ISD);
8. Eye diameter measured to 0.1 mm along the midline of eye from anterior to posterior edge (Eye);
9. Width of the basal rattle segment, measured in 0.1 mm along dorsal-ventral axis of rattle (BRW);
10. Middle blotch length measured in 0.1 mm from the anterior to posterior border of the middle dorsal blotch along vertebral line (MBL);
11. Posterior middle blotch interspace measured in 0.1 mm as the length of the interspace immediately posterior to the middle dorsal blotch along vertebral line (MBI);
12. Number of ventral scales (Vent);
13. Number of subcaudal scales (SubC);
14. Number of dorsal scale rows at midbody (DSR);
15. Number of rattle-fringe scales (RFS);
16. Average number of supralabial scales on the left and right side of the head (SLab);
17. Average number of infralabial scales on the left and right side of the head (ILab);
18. Number of scales in the prefrontal region, including all scales anterior to the supraoculars but excluding the internasals (PreF);
19. Number of interrictal scales (Irict)—counted as the number of dorsal head scale rows between each rictus, excluding ultimate supralabials;
20. Number of dorsal body blotches (DBB)—interconnected blotches counted as one except for three or more, which were counted separately;
21. Number of tail bands (TB)—interconnected bands counted as one except for three or more, which were counted separately;
22. Condition of dorsal blotch borders (SBB)—described as distinct, indistinct, or absent.